Bull. Chem. Soc. Jpn., 76, 1589–1594 (2003)

Template Synthesis of Copper Complexes of Dinucleating and Tetranucleating Macrocyclic Ligands

Kohta Matsumoto, Keisuke Arimura, Masaaki Ohba, and Hisashi Ōkawa*

Department of Chemistry, Faculty of Science, Kyushu University, Hakozaki 6-10-1, Higashiku, Fukuoka 812-8581

(Received February 17, 2003)

The reaction of *N*,*N*′-dimethyl-*N*,*N*′-trimethylenedi(3-aminomethyl-5-methylsalicylaldehydato)copper(II) with 1,3-diaminopropane in DMF afforded the [1 + 1] condensation product [Cu(L)] and the [2 + 2] condensation product [Cu_2(R)]. The dinucleating macrocyclic ligand $(L)^{2-}$ has one N(amine)$_2$O$_2$ and one N(imine)$_2$O$_2$ metal-binding sites sharing two phenolic oxygen atoms and the tetranucleating macrocyclic ligand $(R)^{4-}$ has two N(amine)$_2$O$_2$ and two N(imine)$_2$O$_2$ sites in an alternate arrangement in the macrocyclic framework. The mixture of [Cu(L)] and [Cu_2(R)] was treated with $CuCl_2$ to give [Cu_2(L)Cl_2] (**1a**) and [Cu_4(R)Cl_4] (**2a**), which were separated based on different solubility in methanol. **1a** and **2a** were converted into [Cu_2(L)](ClO_4)$_2$ (**1b**) and [Cu_4(R)(dmf)$_2$](ClO_4)$_4$•2H_2O (**2b**), respectively, by the treatment with $AgClO_4$. **1a** and **1b** each has a dinuclear core doubly bridged by the phenolic oxygen atoms. The crystal structure of [Cu_4(R)(dmf)$_2$](ClO_4)$_4$•2DMF•H_2O•PrOH (PrOH = 2-propanol) (**2b′**) was determined by X-ray crystallography. It has a dimer-of-dimers structure where each N(amine)$_2$O$_2$ entity accommodates one Cu ion in the usual tetradentate chelating mode, whereas each N(imine)$_2$O$_2$ entity assumes a spread shape to combine one Cu ion with its NO donor atoms and another Cu ion with the remaining NO donor atoms. **2b** can be converted into **2a** in the presence of chloride ion. Based on magnetic and visible spectral studies, **2a** is supposed to have a folded structure of **2b** with two Cu–Cl–Cu linkages.

In the past three decades there have been extensive studies on binuclear metal complexes using macrocyclic compartmental ligands derived from 2,6-diformyl-4-methylphenol and diamines.[1] The focus in these works is placed on electrochemical properties,[2] intramolecular electron-transfer,[3] electronic structure of mixed-valence states,[3] magneto-structural correlation,[4] or selective substrate binding[5] of bimetallic systems. Recent attention is directed to the organization of three or more metal centers in predetermined arrays using polynucleating macrocyclic ligands. For example, tetranuclear Ni(II) and Zn(II)[6] and hexanuclear Cu(II)[7] complexes have been obtained by the [2 + 2] or [3 + 3] condensation between 2,6-diformyl-4-methylphenol and 2,6-bis(aminomethyl)-4-methylphenol in the presence of a metal ion. Furthermore, the [2 + 2] condensation product between 2,6-diformyl-4-methylphenol and 1,5-diamino-3-pentanol has been used to produce tetra-, octa- and dodecanuclear Cu(II) complexes.[6,8,9]

The tetranucleating macrocyclic ligand $(R')^{4-}$ (Scheme 1, A) has dissimilar N(amine)$_2$O$_2$ and N(imine)$_2$O$_2$ metal-binding sites in an alternate fashion in a macrocyclic framework. It was first obtained as [Cu_2(R′)], together with [Cu(L′)] of the dinucleating macrocyclic ligand $(L')^{2-}$, by the condensation between *N*,*N*′-dimethyl-*N*,*N*′-ethylenedi(3-aminomethyl-5-bromosalicylaldehydato)copper(II) and ethylenediamine.[10] [Cu_2(R′)] has been used to produce mixed-metal $M^{II}_2Cu^{II}_2$ complexes, [M_2Cu_2(R′)Cl_4], of a deficient double-cubane structure (M = Ni) or a dimer-of-dimers structure (M = Co, Zn).[11]

As an extension of this work, we are interested in the complexation behavior of larger macrocyclic analogs of $(R')^{4-}$. For this purpose *N*,*N*′-dimethyl-*N*,*N*′-trimethylenedi(3-aminomethyl-5-methylsalicylaldehyde (H_2L^{pro}; Scheme 1, B)[12] is chosen as the proligand in this work. Its mononuclear Cu(II) complex, [Cu(L^{pro})], was condensed with 1,3-diaminopropane affording the [2 + 2] condensation product, [Cu_2(R)], together with the [1 + 1] condensation product, [Cu(L)]. [Cu(L)] and [Cu_2(R)] were converted into dinuclear [Cu_2(L)Cl_2] (**1a**) and tetranuclear [Cu_4(R)Cl_4] (**2a**), respectively, by the treatment with $CuCl_2$. Furthermore, **1a** and **2a** were converted into [Cu_2(L)](ClO_4)$_2$ (**1b**) and [Cu_4(R)(dmf)$_2$](ClO_4)$_4$ (**2b**), respectively, by the treatment with $AgClO_4$. Our main focus is placed on how the core structure of **2a** and **2b** varies due to the change of the counter ion.

Experimental

Physical Measurements. Elemental analyses of C, H, and N were obtained at the Elemental Analysis Service Center of Kyushu University. Metal analyses were made on a Shimadzu AA-660 atomic absorption/flame emission spectrometer. Infrared spectra were recorded on a Perkin Elmer BX FT-IR system using KBr disk. Electronic absorption spectra in methanol and reflectance spectra on powdered sample were recorded in methanol on a Shimadzu UV-3100PC spectrometer. FAB mass spectrometric studies were carried out on a JEOL JMS-SX/SX 102A tandem mass spectrometer using *m*-nitrobenzylalcohol as the matrix. Magnetic susceptibilities were measured on a Quantum Design MPMS2 SQUID susceptometer.

Preparation. The synthesis of H_2L^{pro} is described in our previous paper.[12] Other chemicals were purchased from commercial sources and used without further purification.

[Cu(L^{pro})]. H_2L^{pro} (2.07 g, 5.21 mmol) was dissolved in aqueous solution of KOH (0.59 g, 10.5 mmol). To this solution was

Published on the web August 15, 2003; DOI 10.1246/bcsj.76.1589

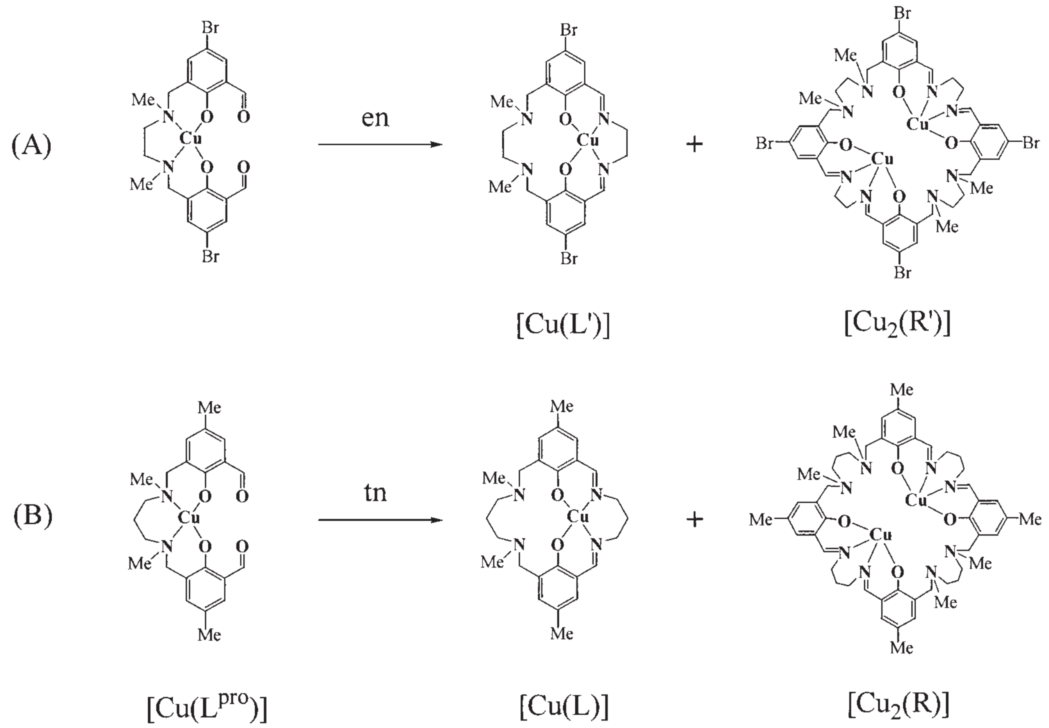

Scheme 1. The synthetic scheme (A) for [Cu(L′)] and [Cu$_2$(R′)] and that (B) for [Cu(L)] and [Cu$_2$(R)].

added an aqueous solution of copper(II) acetate monohydrate (1.04 g, 5.21 mmol) to give a green precipitate. It was thoroughly washed with water and dried in vacuo. The yield was 2.33 g (74.9%). Found: C, 59.89; H; 6.14; N, 6.05; Cu, 13.44%. Calcd for $C_{23}CuH_{28}N_2O_4$: C, 60.05; H, 6.13; N, 6.09; Cu, 13.81%. Selected IR data (ν/cm^{-1}) using KBr disk: 1656, 1611, 1467.

[Cu(L)] and [Cu$_2$(R)]. To a solution of [Cu(L^{pro})] (1 g, 2.17 mmol) in DMF (30 cm^3) was added a solution of 1,3-diaminopropane (0.16 g, 2.17 mmol) in DMF (20 cm^3), and the mixture was refluxed for one hour to give a greenish brown precipitate. The yield was 0.74 g. This was proved to be a mixture of the [1:1] condensation product, [Cu(L)], and the [2:2] condensation product, [Cu$_2$(R)], based on FAB mass spectrometric studies.

[Cu$_2$(L)Cl$_2$] (1a) and [Cu$_4$(R)Cl$_4$] (2a). The mixture of [Cu(L)] and [Cu$_2$(R)] (1 g) was suspended in acetonitrile (50 cm^3). To this was added a solution of copper(II) chloride dihydrate (0.5 g) in methanol (50 cm^3), and the whole was stirred under reflux for one hour. The resulting yellowish green precipitate (complex **A**) was collected and thoroughly washed with methanol (Yield 0.17 g). Anal Found: C, 49.08; H, 5.50; N, 8.79; Cu, 20.29%. Calcd for [Cu$_4$(R)Cl$_4$] ($C_{52}Cl_4Cu_4H_{68}N_8O_4$): C, 49.37; H, 5.42; N, 8.86; Cu, 20.09%. Selected IR (ν/cm^{-1}) using KBr: 1628, 1571, 1464. UV-vis: 340, 480 and 700–1000 nm on powdered sample and 348 (ε: 8500 M^{-1} cm^{-1}), 475 (4600) and 667 (1270) nm in methanol.

The solution separated from complex **A** was concentrated to ca. 30 cm^3 to give green crystals (complex **B**) (Yield 0.96 g). Anal Found: C, 49.76; H, 5.52; N, 8.24; Cu, 20.28%. Calcd for [Cu$_2$(L)Cl$_2$] ($C_{26}Cl_2Cu_2H_{34}N_4O_2$): C, 49.37; H, 5.42; N, 8.86; Cu, 20.09%. Selected IR (ν/cm^{-1}) using KBr: 1630, 1574, 1467. UV-vis: 480 and 700–1000 nm on powdered sample and 600–1000 nm (ε_{max}: 870 M^{-1} cm^{-1} at 650 nm) in methanol.

Complexes **A** and **B** have been confirmed to be [Cu$_4$(R)Cl$_4$] and [Cu$_2$(L)Cl$_2$], respectively, as discussed later.

Table 1. Crystallographic Parameters of [Cu$_2$(L)Cl$_2$] (**1a**) and [Cu$_4$(R)(dmf)$_2$](ClO$_4$)$_4$·2DMF·H$_2$O·PrOH (**2b′**)

	1a	**2b′**
Formula	$C_{26}H_{34}N_4O_2Cl_2Cu_2$	$C_{67}H_{104}N_{12}O_{26}Cl_4Cu_4$
Formula weight	632.58	1889.62
Crystal color	green	green
Crystal system	monoclinic	triclinic
Space group	$P2_1/n$ (#14)	$P\bar{1}$ (#2)
a/Å	15.259(2)	9.9325(9)
b/Å	10.894(2)	14.9718(5)
c/Å	16.192(1)	15.4078(7)
α/°	—	74.213(6)
β/°	100.185(8)	82.639(6)
γ/°	—	83.474(5)
V/Å^3	2649.2(6)	2179.2(3)
Z value	4	1
D_{calc}/g cm^{-3}	1.586	1.44
p-factor	0.065	0.100
No. of reflections	6090 (all)	4945 ($I > 1.50\sigma(I)$)
$R1$	0.060	0.101
R_W	0.177	0.217

[Cu$_2$(L)](ClO$_4$)$_2$·2H$_2$O (1b). To a solution of complex **B** (100 mg) in DMF (10 cm^3) was added AgClO$_4$ (90 mg) and the mixture was stirred at ambient temperature. Resulting AgCl was separated by filtration, and the filtrate was concentrated to a small portion to give green microcrystals. This was proved to be the same compound reported previously.[12]

$[Cu_4(R)(dmf)_2](ClO_4)_4 \cdot 2H_2O$ (2b). To a suspension of complex **A** (100 mg) in DMF (10 cm^3) was added $AgClO_4$ (90 g), and the mixture was stirred at ambient temperature for one hour. Resulting AgCl was separated by filtration and the filtrate was concentrated to a small portion to give $[Cu_4(R)(dmf)_2](ClO_4)_4 \cdot 2H_2O$ as green microcrystals. The yield was 60 mg. Found: C, 41.11; H, 5.21; N, 8.36; Cu, 15.61%. Calcd for $C_{58}Cl_4Cu_4H_{86}N_{10}O_{24}$: C, 40.89; H, 5.09; N, 8.22; Cu, 14.92%. Selected IR (ν/cm^{-1}) using KBr: 1660, 1628, 1573, 1464, 1088. UV-vis: 648 (ε: 980 $M^{-1}\,cm^{-1}$) in DMF.

X-Ray Structure Analyses. The crystal structures of $[Cu_2(L)Cl_2]$ (**1a**) and $[Cu_4(R)(dmf)_2](ClO_4)_4 \cdot 2DMF \cdot H_2O \cdot PrOH$ (PrOH = 2-propanol) (**2b′**) have been determined (Table 1). All measurements for **1a** were made on a Rigaku AFC7R diffractometer with graphite monochromated Mo-Kα radiation and a rotating anode generator. Cell constants and an orientation matrix for data collection were obtained using 25 reflections in the range of $29.24 < 2\theta < 30.00°$. The data were collected at 23 ± 1 °C using the ω-2θ scan technique to a maximum 2θ value of 55.0°. The weak reflections ($I < 10.0\rho(I)$) were rescanned (maximum 4 scans) and the counts were accumulated to ensure good counting statistics. The diameter of the incident beam collimator was 5.0 mm and the crystal-to-detector distance was 235 mm. The computer-controlled slits were set to 9.0 mm (horizontal) and 13.0 mm (vertical).

6090 reflections of 6654 observed ones were unique ($R_{int} = 0.050$). The intensities of three representative reflections were measured after every 150 reflections. Over the course of data collection, the standards decreased by 0.7%. A linear correction factor was applied to the data to account for the phenomenon. The linear absorption coefficient, μ, for Mo-Kα radiation is 18.4 cm^{-1}. An empirical absorption correction based on azimuthal scans of several reflections was applied which resulted in transmission factors ranging from 0.73 to 1.00.

The structure was solved by direct method and expanded using Fourier techniques. The non-hydrogen atoms were refined anisotropically. Hydrogen atoms were included but not refined.

All measurements for **2b′** were made on a Rigaku RAXIS-RAPID Imaging Plate diffractometer with graphite monochromated Mo-Kα radiation. Indexing was performed from 3 oscillations which were exposed for 2.5 minutes. Readout was performed in the 0.200 mm pixel mode. The data were collected at 23 ± 1 °C to a maximum 2θ value of 55.0°. A total of 66 images, corresponding to 222.0° oscillation angles, were collected with two different goniometer settings. Exposure time was 3.00 min per degree. The camera radius was 127.40 mm.

9233 reflections of 15849 observed ones were unique ($R_{int} = 0.069$); equivalent reflections were merged. The linear absorption coefficient, μ, for Mo-Kα radiation is 11.6 cm^{-1}. A symmetry-related absorption correction using the program ABSCOR was applied, which resulted in transmission factors ranging from 0.82 to 0.94. The data were corrected for Lorentz and polarization effects.

The structure was solved by direct method and expanded using Fourier techniques. Non-hydrogen atoms were refined anisotropically except for the H_2O and 2-PrOH molecules in the lattice; these molecules were refined isotropically. Hydrogen atoms were included but not refined.

Crystallographic data have been deposited at the CCDC, 12 Union Road, Cambridge CB2 1EZ, UK and copies can be obtained on request, free of charge, by quoting the publication citation and deposition numbers CCDC 203171.

Results and Discussion

Preparation. In the previous work[12] the reaction of the dinuclear copper complex of the proligand, $[Cu_2(L^{pro})](ClO_4)_2$, with a α,ω-diamine afforded preferentially the [1 + 1] condensation product, $[Cu_2(L)](ClO_4)_2$. This is probably because the two formyl groups in $[Cu_2(L^{pro})](ClO_4)_2$ are fixed in close proximity so as to be efficiently cyclized with one diamine. In this work, mononuclear $[Cu(L^{pro})]$ was used in the reaction with 1,3-diaminopropane. $[Cu(L^{pro})]$ has the Cu ion in the $N(amine)_2O_2$ site as judged from the formyl ν(C=O) vibration at 1665 cm^{-1}.[13] The formyl groups are free from coordination and can rotate about the C(ring)–CHO bond, affording an opportunity of the [2 + 2] condensation with 1,3-diaminopropane. In fact a green product obtained by the reaction of $[Cu(L^{pro})]$ with 1,3-diaminopropane was found to be a mixture of the [1 + 1] and [2 + 2] condensation products, [Cu(L)] and $[Cu_2(R)]$, based on FAB mass spectrometric studies (Scheme 1, B). FAB mass ion peaks centered around $m/z = 995$–1000 correspond to $\{Cu_2(R)\}^+$ and more intense ion peaks centered around $m/z = 498$ correspond to $\{Cu(L)\}^+$. At this stage we were unsuccessful in separating the two products.

The mixture of [Cu(L)] and $[Cu_2(R)]$ was treated with an excess of $CuCl_2$ to give a mixture of $[Cu_2(L)Cl_2]$ (**1a**) and $[Cu_4(R)Cl_4]$ (**2a**). In this treatment, less soluble $[Cu_4(R)Cl_4]$ (**2a**) deposited as a brown precipitate. FAB mass spectrometric studies for **2a** clearly demonstrate that this is a tetranuclear copper complex of $(R^2)^{4-}$; the ion peaks at $m/z = 1155$–1163, 1190–1119 and 1225–1235 correspond to $\{Cu_4(R^2)Cl\}^+$, $\{Cu_4(R^2)Cl_2\}^+$ and $\{Cu_4(R^2)Cl_3\}^+$, respectively. $[Cu_2(L)Cl_2]$ (**1a**) was isolated as green crystals from the solution separated from **2a**.

The chloro complexes, **1a** and **2a**, were then converted into the perchlorate salts, $[Cu_2(L^2)](ClO_4)_2$ (**1b**) and $[Cu_4(R^2)](ClO_4)_4$ (**2b**), respectively, by the treatment with $AgClO_4$. **1b** was previously obtained by the reaction between $[Cu_2(L^{pro})](ClO_4)_2$ and 1,3-diaminopropane.[12] It is also confirmed that $[Cu_4(R^2)](ClO_4)_4$ (**2b**) is converted into $[Cu_4(R)Cl_4]$ (**2a**) when treated with excess NH_4Cl in methanol.

$[Cu_2(L)Cl_2]$ (1a). The crystal structure of **1a** has been determined by X-ray crystallography. An ORTEP drawing is given in Fig. 1 together with the atom numbering scheme. The selected bond distances and angles are given in Table 2.

It has a usual dinuclear structure with two Cu^{II} ions in the $N(amine)_2O_2$ and $N(imine)_2O_2$ sites. The interatomic Cu–Cu separation is 3.070(1) Å. The Cu(1) in the $N(amine)_2O_2$ site has a square-pyramidal geometry together with a chloride ion at an apical site. The in-plane Cu-to-donor distances range from 1.989(5) Å to 2.051(6) Å. The axial Cu(1)-Cl(1) bond distance (2.486(2) Å) is elongated owing to the Jahn-Teller effect of the d^9 electronic configuration. The two methyl groups (C(9) and C(13)) attached to the amine nitrogen atoms (N(1) and N(2)) are situated cis with respect to the basal plane. Such cis arrangement of two N-methyl groups is common for complexes of L^{2-} and related macrocyclic ligands.[12,14–18] The Cl(1) is situated trans to the two N-methyl groups. The Cu is 0.344(3) Å displaced from the basal least-squares plane to-

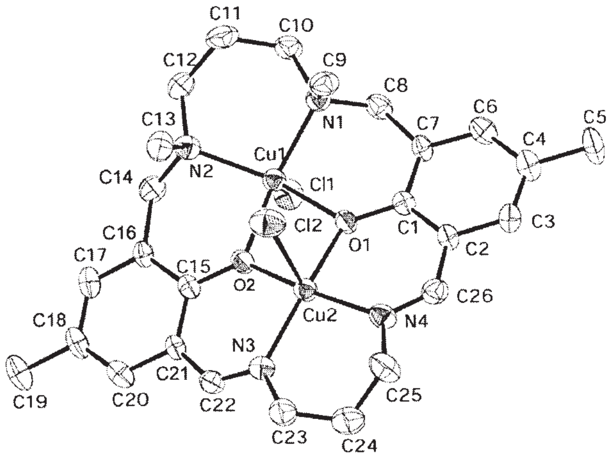

Fig. 1. An ORTEP view of $[Cu_2(L)Cl_2]$ (**1a**).

Table 2. The Selected Bond Distances and Angles of $[Cu_2(L)Cl_2]$ (**1a**)

Bond distances/Å			
Cu(1)–Cl(1)	2.488(2)	Cu(1)–O(1)	2.001(4)
Cu(1)–O(2)	1.993(4)	Cu(1)–N(1)	2.025(5)
Cu(1)–N(2)	2.053(5)	Cu(2)–Cl(2)	2.544(2)
Cu(2)–O(1)	1.987(4)	Cu(2)–O(2)	1.975(4)
Cu(2)–N(3)	1.995(5)	Cu(2)–N(4)	1.973(5)
Bond angles/°			
Cl(1)–Cu(1)–O(1)	104.0(1)	Cl(1)–Cu(1)–O(2)	100.7(1)
Cl(1)–Cu(1)–N(1)	99.1(1)	Cl(1)–Cu(1)–N(2)	96.6(1)
O(1)–Cu(1)–O(2)	76.2(2)	O(1)–Cu(1)–N(1)	88.7(2)
O(1)–Cu(1)–N(2)	156.7(2)	O(2)–Cu(1)–N(1)	157.5(2)
O(2)–Cu(1)–N(2)	89.4(2)	N(1)–Cu(1)–N(2)	98.8(2)
Cl(2)–Cu(2)–O(1)	94.9(1)	Cl(2)–Cu(2)–O(2)	94.1(1)
Cl(2)–Cu(2)–N(3)	102.8(2)	Cl(2)–Cu(2)–N(4)	98.4(2)
O(1)–Cu(2)–O(2)	76.9(2)	O(1)–Cu(2)–N(3)	159.4(2)
O(1)–Cu(2)–N(4)	91.7(2)	O(2)–Cu(2)–N(3)	91.1(2)
O(2)–Cu(2)–N(4)	163.8(2)	N(3)–Cu(2)–N(4)	96.1(2)
Cu(1)–O(1)–Cu(2)	100.6(2)	Cu(1)–O(2)–Cu(2)	101.3(2)

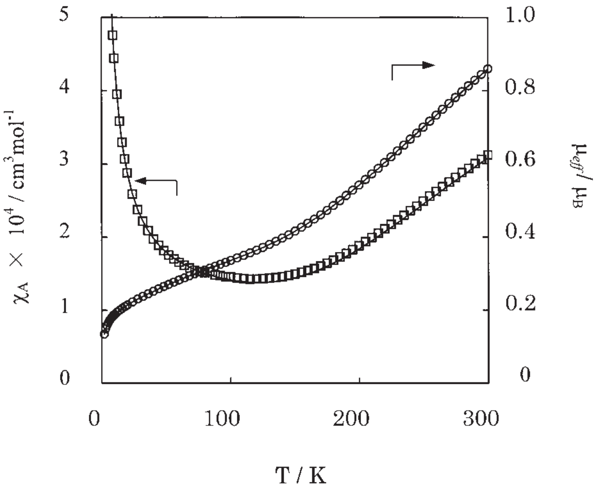

Fig. 2. The temperature-dependence of magnetic susceptibility and magnetic moment of $[Cu_2(L)Cl_2]$ (**1a**).

ward Cl(1).

The geometry about Cu(2) in the iminic site is also square-pyramidal with a chloride ion at an apical site. The in-plane Cu-to-donor bond distances range from 1.971(6) Å to 1.991(6) Å. The axial Cu(2)–Cl(2) distance is 2.544(2) Å. The Cu(2) is 0.273(3) Å displaced from the basal least-squares plane toward Cl(2). The Cl(1) attached to Cu(1) and the Cl(2) attached to Cu(2) are situated trans to each other with respect to the mean molecular plane.

The reflectance spectrum of **1a** has an intense band near 350 nm, a discernible shoulder near 480 nm and a broad envelope at 700–1000 nm. The intense band at ~350 nm is associated with the π–π* transition of the azomethine group.[19,20] The band at ~480 nm can be assigned to a charge-transfer band from Cl^- to Cu^{2+}.[15] A broad envelope in the visible region is ascribed to the superposition of d–d transitions of the Cu(1) and Cu(2) chromophores. The absorption spectrum of **1a** in methanol has two distinct bands at 348 and 650 nm. This spectrum resembles the spectrum of **1b** in DMF (bands at 346 and 640).[12] Evidently, the axial chloride groups of **1a** are liberated in solution.

The magnetic moment of **1a** at room temperature is 0.87 μ_B (per Cu) and the moment decreased with decreasing temperature to 0.17 μ_B at 2 K (Fig. 2). The result implies a strong antiferromagnetic interaction between two Cu ions. An increase in χ_A at low temperature suggests a contamination of a paramagnetic impurity. Magnetic analyses have been carried out using the modified Bleaney-Bowers equation:[21]

$$\chi_A = (1-\rho)\{Ng^2\beta^2/k(T-\theta)\}[3+\exp(-2J/kT)]^{-1} + \rho\{Ng^2\beta^2/4kT\} + N\alpha \qquad (1)$$

where ρ is the fraction of paramagnetic impurity and the other symbols have their usual physical meanings. The cryomagnetic property of **1a** is well reproduced by this equation using $g = 2.10$, $J = -335\ \mathrm{cm}^{-1}$, $N\alpha = 100 \times 10^{-6}\ \mathrm{cm}^3\ \mathrm{mol}^{-1}$, $\theta = -2.0$ K and $\rho = 0.01$. Such a strong antiferromagnetic interaction is observed for di(μ-phenolato)dicopper(II) complexes when two Cu(II) ions form a coplanar dinuclear core.[22–24] A slightly smaller exchange integral of $J = -270\ \mathrm{cm}^{-1}$ is reported for **1b**.[12]

$[Cu_4(R)Cl_4]$ (2a) and $[Cu_4(R)(dmf)_2](ClO_4)_2$ (2b). We have not yet succeeded in preparing single crystals of **2a** suitable for X-ray structure analysis. Single crystals of $[Cu_4(R)(dmf)_2](ClO_4)_4 \cdot 2DMF \cdot H_2O \cdot PrOH$ (**2b′**) were grown when a DMF solution of **2b** was diffused with 2-propanol. The crystallographic result is not complete enough due to the poor quality of the crystal used, but relevant structural discussion is possible. An ORTEP view of **2b′** is given in Fig. 3, together with the atom numbering scheme. Selected bond distances and angles are summarized in Table 3.

The molecule has a dimer-of-dimers structure with the tetranucleating macrocyclic ligand in a rare coordination mode. Each $N(amine)_2O_2$ entity of the ligand accommodates one Cu ion in the usual tetradentate chelating mode, whereas each $N(imine)_2O_2$ entity presumes a spread shape to combine one Cu ion with its NO donor atoms and another Cu ion with the remaining NO donor atoms. The Cu(2) in the aminic site has a square-pyramidal geometry with a dmf oxygen at the apex. The in-plane Cu-to-donor bond distances range from

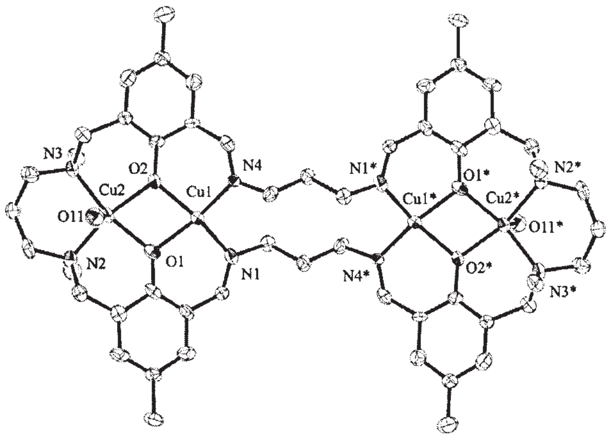

Fig. 3. An ORTEP view of $[Cu_4(R)(dmf)_2](ClO_4)_4 \cdot 2DMF \cdot H_2O \cdot PrOH$ (**2b′**).

Table 3. The Selected Bond Distances and Angles of $[Cu_4(R)(dmf)_2](ClO_4)_4 \cdot 2DMF \cdot H_2O \cdot PrOH$ (**2b′**)

Bond distances/Å			
Cu(1)–O(1)	1.941(7)	Cu(1)–O(2)	1.953(8)
Cu(1)–N(1)	1.963(9)	Cu(1)–N(4)	1.958(8)
Cu(2)–O(1)	1.968(8)	Cu(2)–O(2)	1.992(7)
Cu(2)–O(11)	2.249(8)	Cu(2)–N(2)	2.016(9)
Cu(2)–N(3)	2.011(9)		
Bond angles/°			
O(1)–Cu(1)–O(2)	77.1(3)	O(1)–Cu(1)–N(1)	93.5(3)
O(1)–Cu(1)–N(4)	158.4(3)	O(2)–Cu(1)–N(1)	159.4(3)
O(2)–Cu(1)–N(4)	91.6(3)	N(1)–Cu(1)–N(4)	102.7(3)
O(1)–Cu(2)–O(2)	75.5(3)	O(1)–Cu(2)–O(11)	99.1(3)
O(1)–Cu(2)–N(2)	90.9(3)	O(1)–Cu(2)–N(3)	162.1(3)
O(2)–Cu(2)–O(11)	90.8(3)	O(2)–Cu(2)–N(2)	166.2(3)
O(2)–Cu(2)–N(3)	93.3(3)	O(11)–Cu(2)–N(2)	93.5(3)
O(11)–Cu(2)–N(3)	94.9(3)	N(2)–Cu(2)–N(3)	99.3(4)
Cu(1)–O(1)–Cu(2)	104.1(3)	Cu(1)–O(2)–Cu(2)	102.7(3)

1.965(9) to 2.02(1) Å. The axial Cu–O(dmf) bond is elongated (2.253(10) Å). The Cu(2) is 0.159(8) Å displaced from the basal least-squares plane toward the axial dmf oxygen. The Cu(1) has a planar four-coordinate geometry with the Cu-to-donor bond distances of 1.941(8)–1.96(1) Å. The Cu(1)–Cu(2) interatomic separation is 3.090 Å and the Cu(1)–Cu(1′) separation is 7.435 Å.

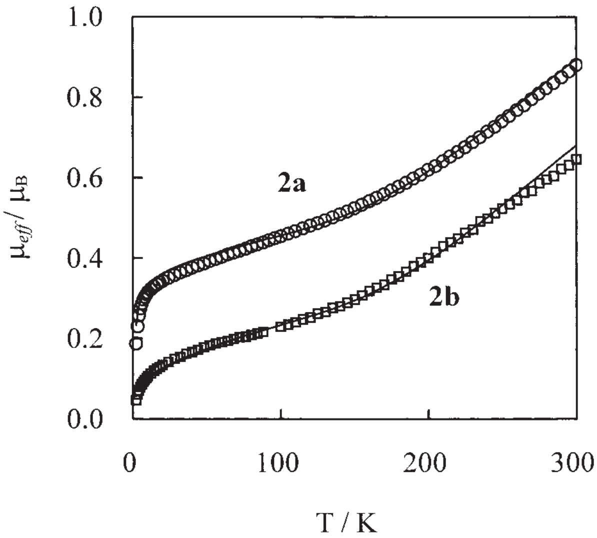

Fig. 4. The temperature-dependence of magnetic susceptibility and magnetic moment of $[Cu_4(R)Cl_4]$ (**2a**) and $[Cu_4(R)(dmf)_2](ClO_4)_4$ (**2b**).

Magnetic properties of **2a** and **2b** have been studied in the temperature range of 2–300 K. The magnetic moment of **2a** is 0.88 μ_B (per Cu) at room temperature and the moment decreased with decreasing temperature to 0.18 μ_B at 2 K (see Fig. 4). The magnetic moment of **2b** is 0.64 μ_B at room temperature and the moment decreased with lowering temperature to 0.05 μ_B at 2 K (Fig. 4).

Magnetic analysis of **2b** is first discussed because its dimer-of-dimers structure is proved. Judged from the significant separation between two dinuclear units, the Bleaney-Bowers equation (Eq. 1) may be applied for magnetic analyses. In fact the magnetic property of **2b** is well reproduced by Eq. 1 using $J = -380$ cm^{-1}, $g = 2.10$, $N\alpha = 60 \times 10^{-6}$ cm^3 mol^{-1}, $\theta = -2.0$ K and $\rho = 0.002$. It is noticed that the cryomagnetic property of **2a** can also be simulated by Eq. 1 using the best-fit parameters of $J = -340$ cm^{-1}, $g = 2.10$, $N\alpha = 100 \times 10^{-6}$ cm^3 mol^{-1}, $\theta = -3.0$ K and $\rho = 0.04$. This fact suggests that **2a** has a tetranuclear core consisting of two magnetically isolated dinuclear units.

In order to gain an insight into the core structure of **2a**, its electronic spectrum has been studied. The reflectance spectrum in the visible region has the Cl-to-Cu LMCT band at ~480 nm and a broad envelope due to the Cu d–d band at 700–1000 nm. The absorption spectrum has absorption bands at 475 and 600–1000 nm. These facts clearly indicate that **2a** has a tetranuclear core with chloride ligation and that the tetranuclear core is stable in methanol. A likely structure of **2a** is a folded form of **2b** with Cu–Cl–Cu linkages (Fig. 5, left). This structure can explain (1) the facile interconversion between **2a** and **2b** by the change of counter ion and (2) the strong chloride ligation in solution. The fact that no appreci-

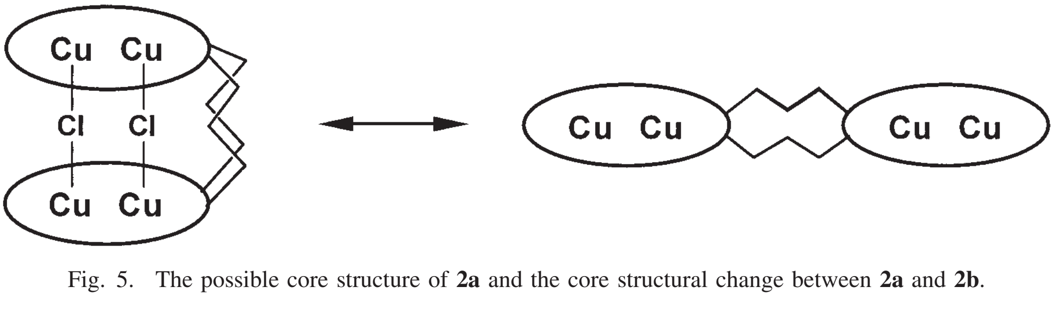

Fig. 5. The possible core structure of **2a** and the core structural change between **2a** and **2b**.

able magnetic interaction occurs between two dinuclear units through the chloride bridges is understandable because the Cu^{2+} has no unpaired electron on its d_{z^2} orbital.

In conclusion the new macrocyclic ligand $(R)^{4-}$ produces tetranuclear Cu complexes of a dimer-of-dimers type whose core structure can vary between a folded form (**2a**) and an open form (**2b**) by the change of the counter ion.

This work was supported by a Grant-in-Aid for Scientific Research on Priority Area 'Metal-assembled Complexes' (No. 10149106), a Grant-in-Aid for COE Research 'Design and Control of Advanced Molecular Assembly System' (No. 08CE2005), and a Grant-in-Aid for Scientific Research Program (No. 13640561) from the Ministry of Education, Culture, Sports, Science and Technology. One of the authors (M. Ohba) thanks Precursory Research for Embryonic Science and Technology (PRESTO), JST for financial support.

References

1 H. Ōkawa, H. Furutachi, and D. E. Fenton, *Coord. Chem. Rev.*, **174**, 51 (1998).

2 S. K. Madal, B. Adhikary, and K. Nag, *J. Chem. Soc., Dalton Trans.*, **1986**, 1175.

3 R. C. Long and D. N. Hendrickson, *J. Am. Chem. Soc.*, **105**, 1513 (1983).

4 S. K. Mandal, L. K. Thompson, K. Nag, J.-P. Charland, and E. Gabe, *Inorg. Chem.*, **29**, 1324 (1990).

5 C. Fraser, L. Johnson, A. L. Rheingold, B. S. Haggerty, G. K. Williams, J. Whelar, and B. Bosnich, *Inorg. Chem.*, **29**, 1324 (1990).

6 A. J. Edwards, B. F. Hoskins, E. H. Kachab, A. Markiewicz, K. S. Murray, and R. Robson, *Inorg. Chem.*, **31**, 3584 (1992).

7 B. F. Hoskins, R. Robson, and P. J. Smith, *J. Chem. Soc., Chem. Commun.*, **1990**, 488.

8 V. McKee and S. S. Tandon, *J. Chem. Soc., Dalton Trans.*, **1991**, 221.

9 S. S. Tandon, L. K. Thompson, and J. N. Beidson, *J. Chem. Soc., Chem. Commun.*, **1992**, 911.

10 M. Yonemura, H. Ōkawa, M. Ohba, D. E. Fenton, and L. K. Thompson, *Chem. Commun.*, **2000**, 817.

11 Y. Nakamura, M. Yonemura, K. Arimura, N. Usuki, M. Ohba, and H. Ōkawa, *Inorg. Chem.*, **40**, 3739 (2001).

12 A. Hori, M. Yonemura, M. Ohba, and H. Ōkawa, *Bull. Chem. Soc. Jpn.*, **74**, 495 (2001).

13 M. Yonemura, Y. Matsumura, M. Ohba, H. Ōkawa, and D. E. Fenton, *Chem. Lett.*, **1996**, 601.

14 M. Yonemura, Y. Matsumura, H. Furutachi, M. Ohba, H. Ōkawa, and D. E. Fenton, *Inorg. Chem.*, **36**, 2711 (1997).

15 M. Yonemura, M. Ohba, K. Takahashi, H. Ōkawa, and D. E. Fenton, *Inorg. Chim. Acta*, **283**, 72 (1998).

16 M. Yonemura, Y. Nakamura, N. Usuki, and H. Ōkawa, *Proc.-Indian Acad. Sci., Chem. Sci.*, **112**, 291 (2000).

17 M. Yonemura, N. Usuki, Y. Nakamura, M. Ohba, and H. Ōkawa, *J. Chem. Soc., Dalton Trans.*, **2000**, 3624.

18 K. Inoue, M. Ohba, and H. Ōkawa, *Bull. Chem. Soc. Jpn.*, **75**, 99 (2002).

19 B. Bosnich, *J. Am. Chem. Soc.*, **90**, 627 (1968).

20 R. S. Downing and F. L. Urbach, *J. Am. Chem. Soc.*, **91**, 5977 (1969).

21 B. Bleaney and K. D. Bowers, *Proc. R. Soc. London, Ser. A*, **214**, 451 (1952).

22 S. L. Lambert and D. N. Hendrickson, *Inorg. Chem.*, **18**, 2683 (1979).

23 H. Ōkawa, M. Tadokoro, Y. Aratake, M. Ohba, K. Shindo, M. Mitsumi, M. Koikawa, M. Tomono, and D. E. Fenton, *J. Chem. Soc., Dalton Trans.*, **1993**, 253.

24 S. Ohtsuka, M. Tadokoro, K. Motoda, M. Ohba, and H. Ōkawa, *J. Chem. Soc., Dalton Trans.*, **1995**, 2599.